

CO₂ Absorption Characteristic of a Type III Porous Liquids Modified by Tetraethylenepentamine

Xingxing Zhao^a, Yudong Ding^{a,b,*}, Lijiao Ma^a, Xun Zhu^{a,b}, Hong Wang^{a,b}, Qiang Liao^{a,b}

^aInstitute of Engineering Thermophysics, School of Energy and Power Engineering, Chongqing University, Chongqing 400030, China.

^bKey Laboratory of Low-grade Energy Utilization Technologies and Systems, Ministry of Education, Chongqing 400030, China.
dingyudong@cqu.edu.cn

The porous liquid (PLs) is a new material containing both permanent porosity of porous materials and liquid fluidity of solvent at room temperature, which has shown a great potential in gas separation. In this study, a novel type III porous liquids were prepared using 2-methylimidazole zinc salt (ZIF-8) modified by tetraethylenepentamine (TEPA) as the main units and 1-Ethyl-3-methylimidazolium Bis(trifluoromethanesulfonyl)-imide ([EMIm][NTf₂]) as the sterically hindered solvent. The effect of amine loading on the CO₂ absorption performance of PLs was investigated. When amine load was 30 wt%, 30TEPA@ZIF-8 not only had the pore structure inside but also effectively increased the CO₂ absorption capacity of PLs. When the effect of different parameters on CO₂ absorption capacity was investigated, it was found that the optimal adsorption temperature was 60 °C, and the optimal concentration of the main units was 7.5 wt%. After five cycles, the absorbent's cycle efficiency and desorption efficiency were more than 98 %. All the results indicate that the prepared PLs in this paper had an application potential in CO₂ capture.

1. Introduction

In recent years, global CO₂ emission has had an upward trend. Despite the influence of COVID-19, the global CO₂ emission in 2020 were still as high as 32 billion tons (BP et al., 2021). The greenhouse effect caused by CO₂ emission has resulted in extreme climates, such as sea-level rise, ocean acidification, glacier melting, et al (WMO., 2021). IPCC has included a temperature rise of 1.5 °C into a target to deal with global warming (IPCC., 2018). For power plants which is the large CO₂ emission sources, CO₂ capture, storage, and utilization technology (CCUS) is considered to be one of the most potential technology for reducing CO₂ emission (Wilberforce et al., 2019). There were four separation technologies, including absorption ((Ochedi et al., 2020), adsorption (Liu et al., 2021) and membrane (Wang et al., 2016) separation, Cryogenic separation (Berstad et al., 2013). Cryogenic separation separates the gas according to the different boiling points of the gas under different pressure and low temperature, it has a high energy consumption at low CO₂ concentration. Membrane separation is suitable for gases with high CO₂ partial pressure, it has a high cost of gas separation owing to the high operating pressure. Absorption was considered to have great potential application in power plants with low CO₂ concentration for CO₂ capture owing to the advantages of continuous operation and large-scale application (Ding et al., 2020). Generally, there were two types of absorbents including physical absorption and chemical absorption. Physical absorption depends on dissolution. CO₂ absorption capacity is affected by pressure and temperature, and it is generally suitable for high pressure and low temperature. Chemical absorption has high CO₂ selectivity and absorption capacity. The absorbent used for flue gas operation in power plant, such as monoethanolamine (MEA), methyldiethanolamine (MDEA), which has a high energy consumption of regeneration, toxicity, strong corrosivity (Wang et al., 2019). Adsorption uses solid absorbents, such as alkaline metal oxides (Li et al., 2021), zeolites (Megias-Sayago et al., 2019), porous carbon (Zhuo et al., 2016), metal-

organic framework materials (Usman et al., 2021). Despite the regeneration consumption was low, the absorbents were difficult to be utilized in power plants with large gas flow. Type III porous liquids is similar to nanofluids which consisting of a solid material with pores and a solvent. It has been demonstrated the main units in the porous liquids could enhance gas adsorption capacity and strengthen mass transfer (Li et al., 2020). In the present work, TEPA modified ZIF-8 as the main units and [EMIm][NTf₂] as the solvent were used for the synthesis of Type III porous liquids. The CO₂ adsorption properties of the PLs were systematically studied.

2. Experimental and methods

2.1 Materials

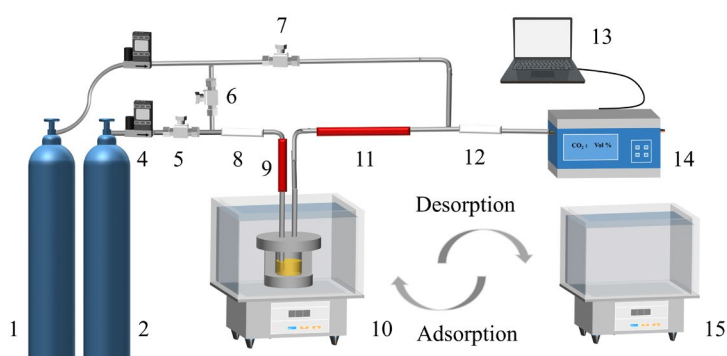
Zinc nitrate hexahydrate (purity of 99 %), Tetraethylenepentamine, and Methanol (purity of 99.5 %) were purchased from Chron Chemicals, China. 2-Methylimidazole (purity of 98 %) and 1-Ethyl-3-methylimidazolium Bis(trifluoromethane sulfonyl)imide ([EMIm][NTf₂]) (purity of 98 %) was purchased from Aladdin, China.

2.2 The synthesis of the Type III porous liquids

The ZIF-8 nanoparticles were synthesized using a solvothermal method (Yang et al., 2014). Subsequently, the x quantity of TEPA was added to 20 mL of methanol and the solution was well mixed. Then, the 2 g of ZIF-8 was added to the solution and the slurry was stirred at room temperature for 6 hours. Finally, the xTEPA-ZIF-8 composite was obtained by vacuum drying at 40 °C. The y-xTEPA-ZIF-8/ILs porous liquids were obtained by dispersing the y proportion of the xTEPA@ZIF-8 into [EMIm][NTf₂] ionic liquids by ultrasonication. The y was the proportion of the TEPA@ZIF-8 composite in the porous liquids and the x was the proportion of TEPA in the TEPA@ZIF-8 composite.

2.3 CO₂ absorption system

The CO₂ absorption system in the present was the bubble reactors shown in Figure 1, which mainly consisted of a gas cylinder, gas pipelines, CO₂ reactor, temperature controlling device, and data acquisition system. The volume fraction of CO₂ was controlled by the gas mass flowmeter, which was 15. vol %, for simulating flue gas. The gas adsorbate was delivered to the gas reactor by pre-heating. In the CO₂ bubbling reactor, CO₂ was adsorbed by absorbents, then the rest of the gas was discharged from the reactor. The volume fraction of CO₂ in the flue gas was detected by the CO₂ infrared gas analyzer and all signals were recorded by the data acquisition system to calculate the CO₂ capacity of adsorbents. When CO₂ in the outlet concentration did not change, it could be considered that the absorption reaches saturation.



1,2: Gas cylinder; 3,4: Gas mass flow controller; 5,6,7: Gas valve; 8,12: Drying tube; 9,11: Heating sleeve; 10: Bubbling reactor; 13: Data acquisition system; 14: CO₂ infrared analyzer; 15: Water bath

Figure1: CO₂ absorption / desorption system

The CO₂ capacity was calculated from the concentration changes during absorption, as shown in Eq(1). Where the C_e was CO₂ saturation absorption capacity, mmol/g. Q_{in} was the mixed gas flow at the inlet, mL/min. x_{in} and x_{out} were the CO₂ percentages at inlet and outlet respectively, vol %. P was the pressure, kPa. T was absolute temperature, K. R was the ideal gas constant. m was the quality of absorbent, g.

$$C_e = \frac{Q_{in}P}{mTR} \int_0^t (x_{in} - \frac{1-x_{in}}{1-x_{out}} x_{out}) dt \quad (1)$$

2.4 CO₂ desorption

The CO₂-saturated absorbent was put into the water bath at a preset temperature, then the desorption process was carried out under an N₂ atmosphere at the flow of 300 mL/min for two hours. The CO₂ volume fraction at the outlet was recorded by the gas infrared analyzer. The analysis was finished until the outlet concentration was not changing. The cycle efficiency, η_e , represented the CO₂ adsorption capacity of the absorbent after cyclic regeneration. Cycle efficiency was calculated by the following Eq(2).

$$\eta_{ei} = \frac{C_{ei}}{C_{e1}} \quad (2)$$

Where η_{ei} was the cycle efficiency at the i time. C_{ei} is the CO₂ desorption amounts at the i th time, mmol/g. C_{e1} was the saturated adsorption amounts, mmol/g.

3. Results and discussion

3.1 The characterization of the TEPA@ZIF-8 composite

Four ratios of TEPA were loaded onto ZIF-8 nanoparticles by impregnations. Thermogravimetric analysis of xTEPA@ZIF-8 composite was carried out using NETZSCH STA 409 PC/PG for testing TEPA load (Figure 1). It was found that there was a weight loss step at 160 °C in the TEPA decomposition curve, indicating the decomposition temperature of TEPA was 160 °C. For ZIF-8 nanoparticles, the weight loss step occurs at around 600 °C. There were existing three weight loss steps in the TEPA@ZIF-8 composites. The first weight loss occurs at 50°C, due to a small amount of methanol being sealed inside the ZIF-8 in the impregnations process. Then the second weight loss step occurs at 160 °C, as TEPA was successfully loaded onto the ZIF-8 nanoparticles. And as the temperature rises to 600 °C, ZIF-8 began to decompose.

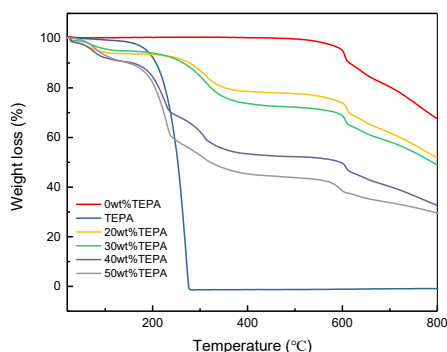


Figure 2: The TG curves of xTEPA@ZIF-8 composite

Table 1: Pore analysis of xTEPA@ZIF-8

materials	BET Specific-surface area (m ² /g)	Pore volume (cm ³ /g)
ZIF-8	1,524.28	0.66
20wt%TEPA@ZIF-8	667.82	0.31
30wt%TEPA@ZIF-8	304.53	0.12
40wt%TEPA@ZIF-8	52.21	0.024
50wt%TEPA@ZIF-8	0.32	0.000052

Subsequently, the specific surface area and pore volume of xTEPA@ZIF-8 composite were obtained using the ASAP 2460 Physical adsorption analyzer (Table 1). It was found that the specific-surface area and pore volume of ZIF-8 nanoparticles decreased with the TEPA load owing to the TEPA blocking the channels in ZIF-8 nanoparticles, and when the TEPA loading reached 40 wt%, the specific-surface area and pore volume drop sharply to 52.21 m²/g and 0.024 cm³/g respectively. The pores in ZIF-8 disappeared completely when continuing

to increase the TEPA load. Weight loss curves were shown (Figure 2). Hence, the 20TEPA@ZIF-8 and 30TEPA@ZIF-8 composites could be used as the main units for the type-III porous liquids.

3.2 The effect of y-xTEPA-ZIF-8 on the CO₂ absorption capacity of the PLs

The effect of the y-xTEPA-ZIF-8 on the CO₂ absorption capacity of the PLs was studied using the bubble reactors. The 15 g of PLs, which contained 5 % mass concentration of y-xTEPA-ZIF-8 was used for CO₂ absorption in fuel gas (Figure 3). It was found that all absorption curves contain two absorption processes including the fast and slow CO₂ absorption process except the ZIF-8/ILs. For ZIF-8/ILs, the CO₂ absorption rate was slow due to CO₂ entering the main liquid phase entering the pores of ZIF-8 by diffusion. Nevertheless, for the TEPA@ZIF-8/ILs PLs, the TEPA was loaded on ZIF-8 nanoparticles and there were existing chemically-reactions, resulting in a rapid absorption rate at the beginning of the CO₂ absorption period. It was also found TEPA in PLs could increase the CO₂ absorption capacity, but not the more TEPA load was the better. TEPA load was 30 wt%, and the PLs have the highest CO₂ absorption capacity, with a value of 0.26 mmol/g. The loading of TEPA occupied the internal channels of ZIF-8 and decreased the specific-surface area of ZIF-8 nanoparticles. Although the specific-surface area of 30TEPA@ZIF-8 was 300 m²/g, which was lower than that of 20TEPA@ZIF-8, 667.82 m²/g, the TEPA in ZIF-8 nanoparticles remained active. At higher TEPA loading levels, there was almost no internal porosity in ZIF-8 nanoparticles. Amounts of TEPA were encapsulated inside ZIF-8 and lost the activation.

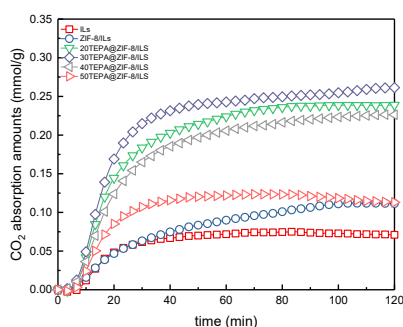


Figure 3: The CO₂ absorption capacity of PLs at different TEPA loads

3.3 The effect of concentration of 30TEPA@ZIF-8 on the CO₂ absorption capacity of the PLs

The CO₂ absorption capacity of PLs at different concentrations of 30TEPA@ZIF-8 at 30 °C, in fuel gas of 200 mL/min was performed in Figure 4. It was found that the concentration of TEPA@ZIF-8 was an important factor dominating the CO₂ absorption capacity of the PLs. On the one hand, the active sites originating from TEPA increased with the concentration of main units. On the other hand, Brownian motion generated by low concentration main units could increase CO₂ mass transfer (Yu et al., 2019). However, the higher concentration of the main unit increased the viscosity of PLs, resulting in the mass transfer resistance increasing (Wang et al., 2015).

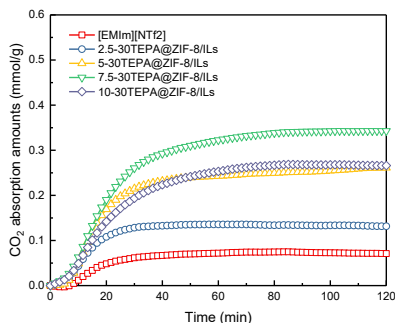


Figure 4: The CO₂ absorption capacity of PLs at different concentrations of 30TEPA@ZIF-8

It was found the CO₂ absorption capacity increased with the concentration of the main unit and then decreased. The maximum absorption capacity was 0.34 mmol/g with a concentration of 7.5 wt%. The main reason was the solvent in the present work was [EMIm][NTf₂] which dissolved CO₂ by physical absorption (Hong et al., 2007). When the concentration of the main units increased, the number of amine groups increased. And there was chemisorption originating from the amine groups in PLs in addition to physical adsorption. It can be found that when the mass concentration increased to 10 wt%, the CO₂ absorption rate and absorption capacity were lower than for a concentration of 7.5 wt%. This was because the viscosity of the PLs had increased, the CO₂ mass transfer resistance increased, resulting in amounts of amine groups were not reacting with CO₂ and the absorption appeared to be pseudo-saturated.

3.4 The effect of the temperature on the CO₂ absorption capacity of the PLs

The CO₂ absorption curves of PLs with 30TEPA@ZIF-8 of 5 wt% at different temperatures are shown in Figure 5. It was found that the CO₂ absorption capacity of PLs increased first and then decreased with temperature, and the optimal absorption temperature was 60 °C and the corresponding CO₂ absorption capacity was mmol/g. It had been concluded that the absorption of porous liquids in the present work includes chemisorption and physisorption from the section. When the temperature increased, the effect of physical adsorption was weakened owing to the increased thermal motion of molecules. When the temperature was increased from 30 °C to 60 °C, the chemical activation energy of the PLs and the activity of the adsorption sites increased, resulting in the enhancement of the chemisorption. When the temperature was 70 °C, as the amine group and CO₂ was exothermic, the high temperature inhibited the reaction of CO₂ with the amine group and caused the reaction to proceed in the direction of CO₂ resolution. Thus, the CO₂ uptake of PLs was reduced at 70 °C.

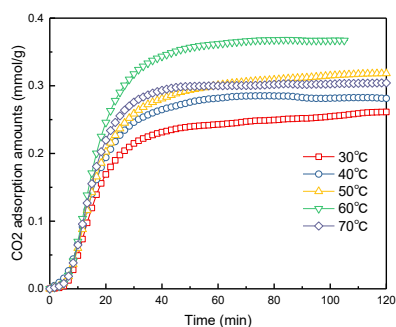


Figure 5: The CO₂ absorption capacity of PLs at different temperature

3.5 The cyclic regeneration performance

The regeneration process was carried out using the thermal regeneration method. Five times regeneration absorption efficiency was performed (Figure 6). After five cycles, the CO₂ absorption capacity was more than 98.0 % of the initial absorption capacity, which indicated that the absorber had good cycling stability and was potential material in carbon capture.

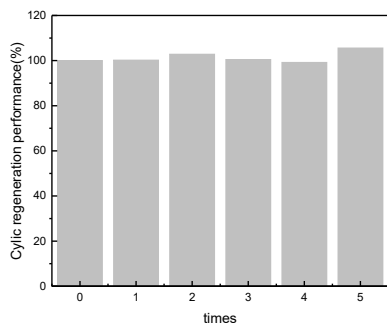


Figure 6: The cyclic regeneration performance of PLs

4. Conclusion

In this paper, TEPA was successfully modified onto ZIF-8 nanoparticles using the impregnation method. Then, the TEPA-modified ZIF-8 nanoparticles were used as the main units, and [EMIm][NTf₂] was used as the site-resistant solvent to synthesize type-III porous liquid. The CO₂ absorption characteristics were tested using the bubble reactors. By studying the effect of different parameters, including temperature, amine load, and concentration of the main unit on CO₂ absorption in porous liquids, it was found that the optimum amine loading was 30 wt%, the optimum adsorption temperature was 60 °C and the optimum concentration of the main unit was 7.5 wt%. PLs showed a good CO₂ adsorption performance after five cycles of regeneration, indicating it had the potential for CO₂ capture.

Acknowledgments

This work was supported by National Natural Science Foundation of China (No.51876013) and Innovative research group project of National Natural Science Foundation of China (No. 52021004).

References

- Berstad D., Anantharaman R., Neksa P., 2013, Low-temperature CO₂ capture technologies - Applications and potential, *International Journal of Refrigeration*. 36(5), 1403-1416.
- BP. 2021, *bp's Statistical Review of World Energy 2021*, London, UK.
- The Intergovernmental Panel on Climate Change. 2018, *Special Report: Global Warming of 1.5°C*, Geneva, Switzerland
- Ding S., 2020, Adsorption of CO₂ from flue gas by novel seaweed-based KOH-activated porous biochars, *Fuel*. 260, 116382.
- Hong G., Jacquemin J., Deetlefs M., Hardacre C., Husson P., Gomes M.F.C., 2007, Solubility of carbon dioxide and ethane in three ionic liquids based on the bis((trifluoromethyl)sulfonyl)imide anion, *Fluid Phase Equilibria*. 257(1), 27-34.
- Li P., Chen R., Lin Y., Li W., 2021, General approach to facile synthesis of MgO-based porous ultrathin nanosheets enabling high-efficiency CO₂ capture, *Chemical Engineering Journal*, 404, 126459.
- Li Y., 2020, *Research Progress of Porous Liquids*, *ChemistrySelect*. 5(43), 13664-13672.
- Liu R.S., Shi X.D., Wang C.T., Gao Y.Z., Xu S., Hao G.P., Chen S.Y., Lu A.H., 2021, Advances in post-combustion CO₂ capture by physical adsorption: from materials innovation to separation practice, *Chemsuschem*, 14(6), 1428-1471.
- Megias-Sayago C., Bingre R., Huang L., Lutzweiler G., Wang Q., Louis B., 2019, CO₂ Adsorption capacities in zeolites and layered double hydroxide materials, *Frontiers in Chemistry*, 7, 00551.
- Ochedi F.O., Yu J., Yu H., Liu Y., Hussain A., 2020, Carbon dioxide capture using liquid absorption methods: a review, *Environmental Chemistry Letters*, 19(1), 77-109.
- World Meteorological Organization. 2021, *State of the Global Climate 2020*, Geneva, Switzerland
- Usman M., Helal A., Abdelnaby M.M., Alloush A.M., Zeama M., Yamani Z.H., 2021, Trends and prospects in UiO-66 metal-organic framework for CO₂ capture, separation, and conversion, *Chemical Record*. 21(7), 1771-1791.
- Wang S.F., Li X.Q., Wu H., Tian Z.Z., Xin Q.P., He G.W., Peng D.D., 2016, Advances in high permeability polymer-based membrane materials for CO₂ separations, *Energy & Environmental Science*, 9(6), 1863-1890.
- Wang T., Yu W., Fang M.X., He H., Xiang Q.Y., Ma Q.H., Xia M.L., Luo Z.Y., Cen K.F., 2015, Wetted-wall column study on CO₂ absorption kinetics enhancement by additive of nanoparticles, *Greenhouse Gases-Science and Technology*, 5(5), 682-694.
- Wang X., Shang D.W., Zeng S.J., Wang Y.M., Zhang X.C., Zhang X.P., Liu J.D., 2019, Enhanced CO₂ capture by binary systems of pyridinium-based ionic liquids and porous ZIF-8 particles, *Journal of Chemical Thermodynamics*, 128, 415-423.
- Wilberforce T., Baroutaji A., Soudan B., Al-Alami A.H., Olabi A.G., 2019, Outlook of carbon capture technology and challenges, *Science of the Total Environment*, 657, 56-72.
- Yang Y., Ge L., Rudolph V., Zhu Z.H., 2014, In situ synthesis of zeolitic imidazolate frameworks/carbon nanotube composites with enhanced CO₂ adsorption, *Dalton Transactions*, 43(19), 7028-7036.
- Yu W., Wang T., Park A.H.A., Fang M.X., 2019, Review of liquid nano-absorbents for enhanced CO₂ capture, *Nanoscale*, 11(37), 17137-17156.
- Zhuo H., Hu Y.J., Tong X., Zhong L.X., Peng X.W., Sun R.C., 2016, Sustainable hierarchical porous carbon aerogel from cellulose for high-performance supercapacitor and CO₂ capture, *Industrial Crops and Products*, 87, 229-235.